Int. J. of GEOMATE, June, 2013, Vol. 4, No. 2 (Sl. No. 8), pp. 546-551
Geotec., Const. Mat. & Env., ISSN:2186-2982(P), 2186-2990(O), Japan

Physical and Mechanical Properties of Sand-Gravel Mixtures Evaluated from DEM Simulation and Laboratory Triaxial Test

Janaka Kumara[1], Kimitoshi Hayano[2], Yuuki Shigekuni[2] and Kota Sasaki[2]
1 Deptmenet of Civil Engineering, Yokohama National University, Japan
2 Department of Urban Innovation, Yokohama National University, Japan

ABSTRACT: In railway tracks, ballast fouling due to fine materials mixing has been identified as a challenging issue. In this research, deformation characteristics of sand-gravel mixtures, simulating fine-ballast mixtures, were studied using laboratory and DEM-simulated triaxial compression tests. The DEM simulations were done in Yade, an open source developed based on DEM. Initially, void ratio characteristics of sand-gravel mixtures were studied. Then, triaxial compression tests were conducted for the specimens of 50% and 80% of relative densities. The void ratio results indicated that, initially, void ratios decreased with %sands. After reaching the minimum void ratios, void ratios increased with %sands. The triaxial test results indicated that, on average, similar behaviour in stress-strain curves, where, at initial %sands, stress-strain curves became higher and then, stress-strain curves became smaller, though it was slightly different in laboratory tests.

Keywords: DEM Simulations, Laboratory Tests, Mechanical Properties, Physical Properties, Sand-Gravel Mixtures

1. INTRODUCTION

In railway tracks, due to repeated heavy train loads, fine materials mix with ballasts. The fine materials come mainly from the underneath layers and to a lesser extent due to particle crushing as well [1]. Changes in deformation properties of ballasts due to sand intrusions have been identified as a major problem in railway engineering. In many cases, ballasts containing sands shows large settlements, which is induced mainly by railway traffic loading. However, degree of settlement depends not only on traffic volume but also on physical and mechanical properties of the ballasts. Though there had been various researches conducted on pure materials of ballasts and fines [2]-[3], there had not been sufficient researches conducted on deformation characteristics of fine-ballast mixtures simulating actual field rail-track conditions. Perhaps, difficulties in simulating multi-size particles in numerical simulations would have been the main issue behind less number of researches on fine-ballast mixtures. However, it is very important to understand effects of fine materials mixing on deformation characteristics of ballast to understand degradation of ballast layers and to propose maintenance works for degraded ballast layers.

After development of DEM [4], DEM simulations became the most widely used numerical method to study deformation characteristics of granular materials. As laboratory experiments are complicated and expensive for various types of field conditions, nowadays, numerical simulations are preferred in many research works. However, laboratory experiments are still required to verify the accuracy of the numerical simulations. In this research, deformation characteristics of granular materials including sand-gravel mixtures were studied using triaxial compression tests in Yade [5] as the numerical method in addition to laboratory triaxial compression tests.

1.1 Yade

Yade is an extensible open-source framework for discrete numerical models, focused on Discrete Element Method [5]. Yade is a 3-D numerical method. In Yade, particle size distribution (PSD) curves of sand-gravel mixture were simulated using gap-graded PSD curves. Widulinski et al. (2009) [6] and Sayeed et al. (2011) [7] have also conducted triaxial compression tests using sphere particles in Yade and found good agreements with experimental results.

2. METHODOLOGY

In this research, since size of ballast (i.e., 10-60mm) is too large to use in triaxial compression test (the specimen size is 100mm in diameter and 200mm in height), gravel of size of 1/5 of actual ballast, was used. Medium size sand was used as the fine material. At the initial stage, void ratio characteristics of sand-gravel mixtures were evaluated using laboratory density tests and DEM triaxial simulations. The density tests were conducted according to JIS A 1204-2009 [8]. In the next stage, deformation characteristics of sand-gravel mixtures were evaluated for the specimens of 50% and 80% of relative densities, D_r. The deformation characteristics were evaluated using both laboratory and DEM simulated triaxial compression tests.

2.1 Laboratory Triaxial Compression Tests

Laboratory triaxial compression tests were conducted using the apparatus shown in Fig. 1 according to JGS 0527 [9]. Axial deformations were measured by an external displacement transducer and a pair of LDTs [10]. However, the measurements of LDTs used to determine small strain deformation properties, are not included in this paper. The triaxial tests were conducted under 80kPa of confining pressure, σ_c. Though railway track ballast is subjected to 30-40kPa of σ_c, the triaxial tests were conducted under 80kPa to minimize errors (e.g., membrane force effects, etc.) arising with small suction pressure.

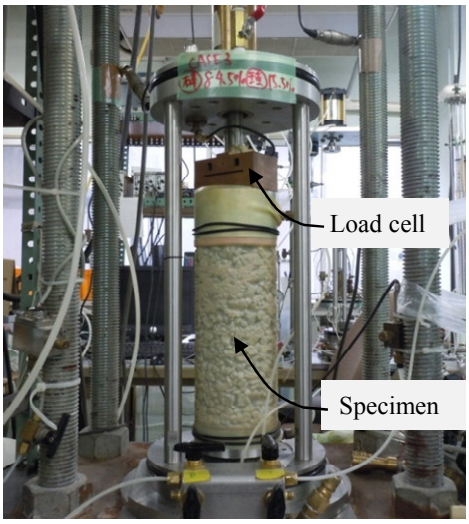

Fig. 1: Triaxial apparatus

2.2 DEM Simulations

In triaxial test simulations, void ratio is determined by friction angle, during isotropic compression, ϕ_c. After maximum and minimum void ratios, e_{max} and e_{min}, of the specimens were determined, void ratios related to 50% and 80% of relative densities, e_{50} and e_{80}, were obtained using Eq. (1). Then, the values of ϕ_c related to e_{50} and e_{80} were determined. In the DEM simulations, particle size was simulated as 100 times larger than the size of laboratory specimens to reduce simulation time. The DEM simulations were done using sphere particles. The input parameters used in the DEM simulations are given in Table 1. Though 5m/s of V_w was used for gravel specimens, smaller values of V_w (1m/s used here) were required for the specimens of small size particles to stabilize the simulations.

Table 1: Input parameters of DEM triaxial simulations

Parameter	Value	Remarks
Stability criterion	0.01	Help to stabilize system
Friction angle of spheres during isotropic compression, ϕ_c	See Table 2	ϕ_c determines void ratio
Coefficient of Cundal non-viscous damping	0.2	Default value
Max. time step, Δt (s)	0.000658	Default value
Density of spheres, ρ_s (kg/m^3)	2600	
Max. velocity of walls, V_w (m/s)	1.0/5.0*	Help to stabilize the system
Number of particles, N	10000	
Confining pressure, σ_c (kPa)	80	
Friction angle of spheres just before shearing, ϕ_s (degree)	30	
Ratio of shear and normal contact stiffness for spheres, K_s/K_n	0.5	
Stiffness of spheres, E_s (MPa)	15	
Strain rate (s^{-1})	0.1	

Note: * Used for gravel specimen

$$D_r = \frac{e_{max} - e}{e_{max} - e_{min}} \times 100(\%) \quad (1)$$

2.3 Sample Preparation

Twelve specimens each (six each for 50% and 80% of D_r) were prepared with different %sands as given in Table 2 for laboratory experiments and DEM simulations.

Table 2: Details of friction angle and void ratio

Sands (%)	Friction angle, ϕ_c (degree)		Void ratio, e	
	D_r = 50%	D_r = 80%	D_r = 50%	D_r = 80%
0	16.5	4.5	0.632	0.566
15	11.8	3.8	0.485	0.429
30	16.3	4.2	0.403	0.342
50	20.0	5.0	0.450	0.396
70	17.15	4.4	0.519	0.460
100	16.4	3.5	0.646	0.574

3. RESULTS AND DISCUSSIONS

Fig. 2 shows PSDs of laboratory specimens. PSDs of the samples were evaluated using sieve analysis test according to JIS A 1204 [11]. Fig. 3 shows PSDs of the DEM simulations. As shown in Fig. 3, particle size of DEM-simulated specimens is 100 times larger than those of laboratory specimens.

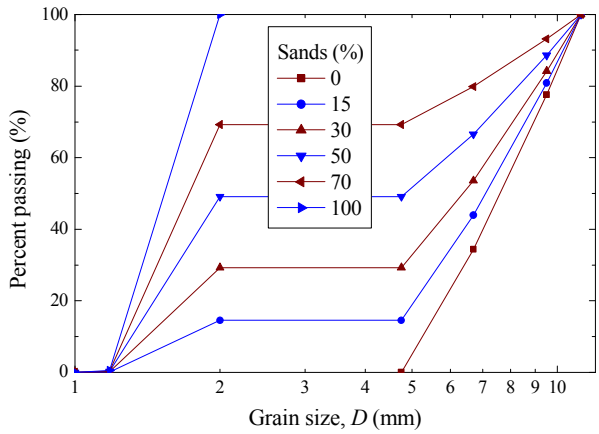

Fig. 2: Particle size distribution of laboratory specimens

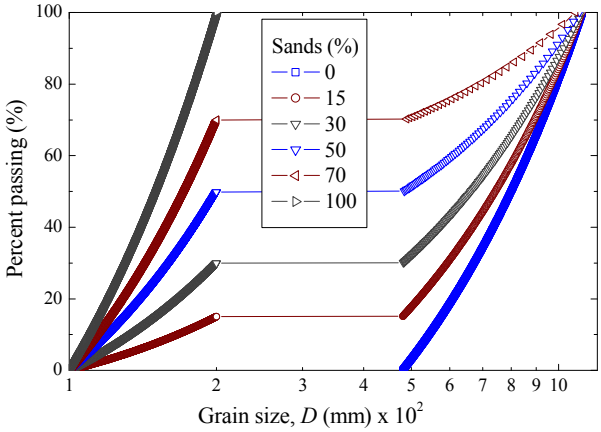

Fig. 3: Particle size distribution of DEM simulated specimens

3.1 Void Ratio Characteristics

Fig. 4 shows relation of void ratio of the specimens with %sands. In Fig. 4, $e_{max,exp}$ and $e_{max,DEM}$ represent maximum void ratios of experimental and DEM-simulated specimens respectively. As shown in Fig. 4, void ratios (both e_{max} and e_{min}) decreased with %sands at initial level, then, after certain percentage of sands, void ratios increased with %sands. The minimum value of void ratios (both e_{max} and e_{min}) reached at 50% and 30% sands for laboratory and DEM-simulated specimens respectively. The difference in percentage of sands to reach minimum value of void ratios should be attribute to differences in particle shape as DEM simulations were done using sphere particles whereas laboratory specimens consist of irregular shape particles. Lade et al. (1998) [12] also showed similar results for binary mixtures of sphere particles where minimum value of void ratios were observed mainly at 20% - 40% fines depending on diameter ratio of the two particles.

The results also showed that void ratios of the DEM-simulated specimens are smaller than laboratory specimens for the specimens of larger particles (e.g., gravel specimen). However, it should be noted that void ratio of the DEM-simulated specimens were measured at the end of isotropic compression (under 80kPa of σ_c) whereas in laboratory specimens, void ratios were measured just after sample preparation (i.e., before test was conducted). As shown in Fig. 4, the difference in void ratios of laboratory and the DEM-simulated specimens become smaller for the specimens of more sands than those of more gravel particles. The large difference in void ratios for the specimens of larger particles should be attribute to different particle shapes in laboratory specimens and DEM simulations. It should also be noted that, in general, gravel particles are angular shape while sand particles are rounded shape. Fig. 5 shows relation of e_{max} and e_{min} for both laboratory and DEM simulated specimens. Fig. 5 clearly shows that both relations are linear with roughly a same gradient (i.e., increasing rate) though experimental data shows higher void ratios. As explained above, smaller void ratios in DEM simulations should be attribute to different particle shapes in the two methods.

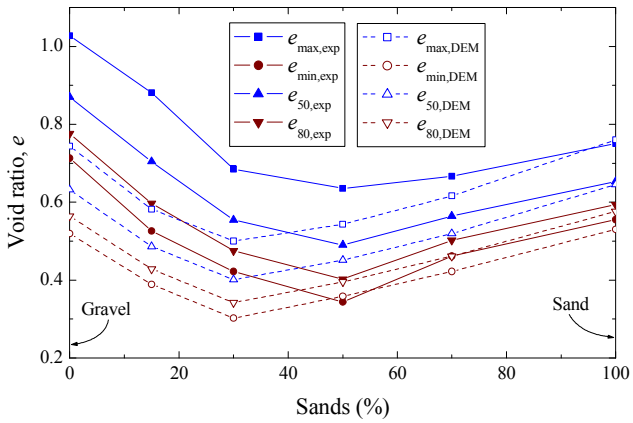

Fig. 4: Void ratio of laboratory and DEM-simulated specimens

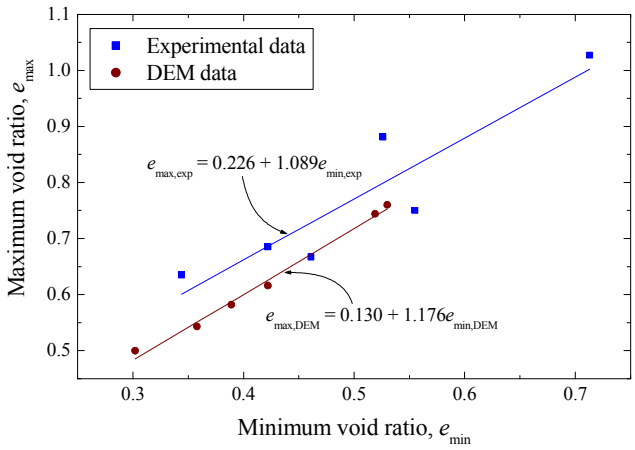

Fig. 5: Comparison of relations of maximum and minimum void ratios

3.2 Triaxial Test Results

Fig. 6 shows a DEM triaxial test simulation at different steps. The specimens were prepared in a box as shown in Fig. 6. As shown in Fig. 6 (a), at the beginning of particle generation, packing is very loose. At the end of isotropic compression, void ratios were obtained to compare with those of laboratory specimens. Fig. 7 shows deviator stress vs. axial strain for laboratory specimens of 50% of D_r. Fig. 8 shows deviator stress vs. axial strain for DEM-simulated specimens of 50% of D_r. As shown in Fig. 7, stress-strain curves became higher with %sands up to 30% sands. Then, stress-strain curves became smaller with %sands. The behaviour of stress-strain curves is similar to those of void ratios, though not for all the cases (e.g., 50% sand case). The difference behaviours of stress-strain curves from void ratios with %sands, should be attribute to different shapes of gravel and sand. As expected, the results also showed that gravel specimen experienced higher stress-strain curve than that of sand specimen. In the DEM simulations, as shown in Fig. 8, stress-strain curves became higher up to 30% sands, same as void ratio decreased with initial %sands. Then, stress-strain curves became smaller same as void ratio increased with %sands. In DEM simulations too, gravel specimen experienced higher stress-strain curve than that of sand specimen. However, it should be noted that laboratory specimens experienced higher stress-strain curves compared to DEM-simulated specimens. The difference in stress-strain curves between the two methods should be attribute to different particle shapes as the DEM simulations consist of sphere particles while laboratory specimens consist of irregular shape particles. Lin and Ng (1997) [13] also showed that irregular shape particles give higher stress-strain curves than those of sphere particles. He compared stress-strain relations for the samples made of ellipsoid and sphere particles and found that ellipsoid particles give higher stress-strain curve. Yan et al. (2009) [14] also studied effects of particle shapes on strength characteristics and found that sphere particles give smaller stress-strain curve compared to clump particles (i.e., irregular shape particles).

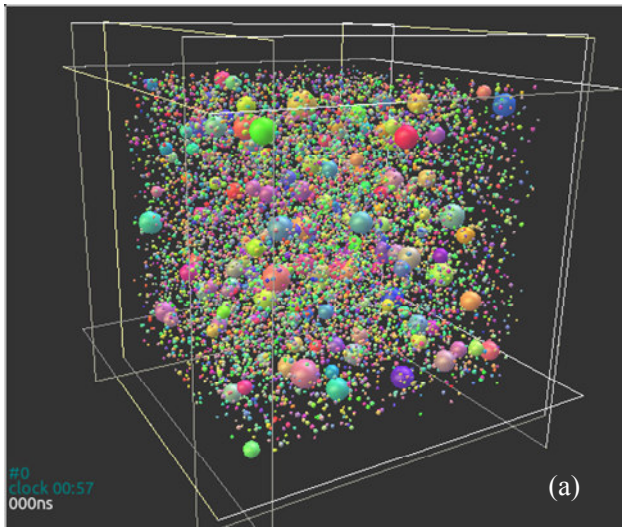

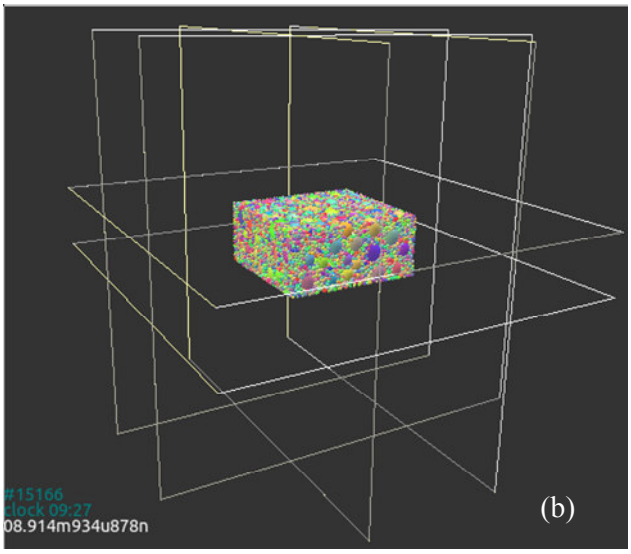

Fig. 6: A DEM triaxial test simulation at the (a) particle generation and (b) end of simulation (30% sand case)

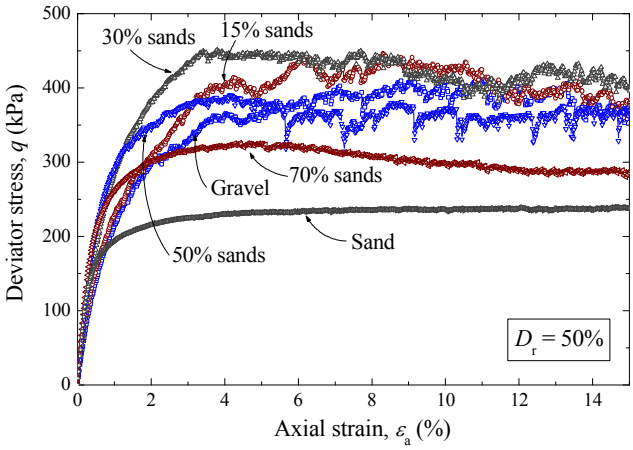

Fig. 7: Deviator stress vs. axial strain from laboratory specimens of 50% of D_r

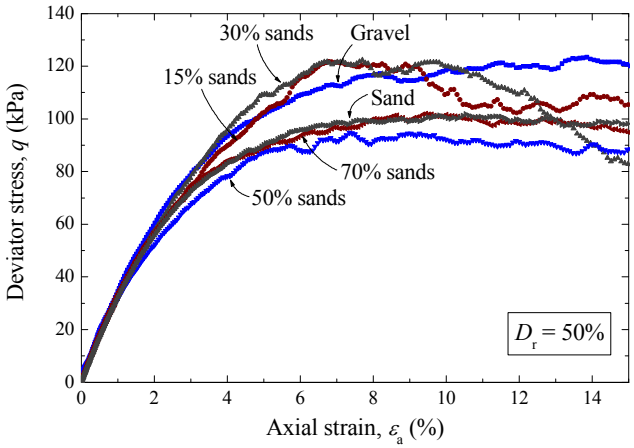

Fig. 8: Deviator stress vs. axial strain from DEM simulations of 50% of D_r

Fig. 9 shows deviator stress vs. axial strain for laboratory specimens of 80% of D_r. Fig. 10 shows deviator stress vs. axial strain for DEM-simulated specimens of 80% of D_r. As shown in Fig. 9, some specimens (i.e., the specimens of 30%, 50% and 70% sands) reached a peak value in stress-strain curves and then stress-strain curves decreased same as a dense specimen. Out of these three specimens, the specimen of 30% sands experienced the highest stress-strain curve. However, gravel specimen experienced the highest stress-strain curve showing stress-strain behaviour of a loose specimen where there is no clear peak value in stress-strain curve. As shown in Fig. 10 for DEM simulations, the specimen of 30% sands experienced the highest stress-strain curve, harmonizing with the minimum void ratio. In 80% of D_r too, gravel specimen experienced higher stress-strain curves than those of sand specimen. In the DEM simulations, the triaxial test results show that sand-gravel specimens of 30% sands experienced the highest stress-strain curves showing the densest packing harmonizing with void ratio results. However, the results from laboratory tests were slightly different.

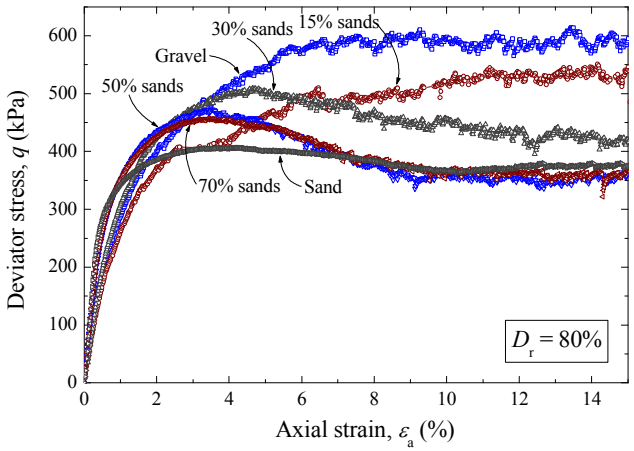

Fig. 9: Deviator stress vs. axial strain from laboratory specimens of 80% of D_r

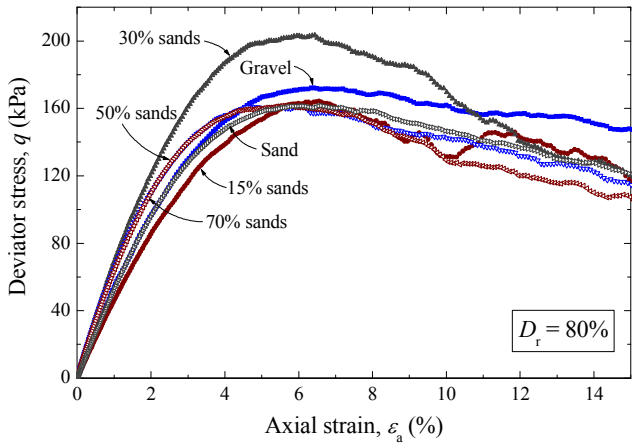

Fig. 10: Deviator stress vs. axial strain from DEM simulations of 80% of D_r

Figs. 11 and 12 show comparisons of deviator stress vs. axial strain between laboratory tests and DEM triaxial test simulations for 50% and 80% of D_r respectively. Though Figs. 11 and 12 do not show a very clear relation of different stress-strain curves for the two specimens (i.e., gravel and 30% sands specimens) for both cases, Fig. 11 showed that the specimen of 30% sands experienced higher stress-strain curve than the gravel specimen from laboratory tests while Fig. 12 showed that the specimen of 30% sands experienced higher stress-strain curve than that of the gravel specimen in DEM simulations. However, it is understood that more tests should be needed for consistent results in both methods.

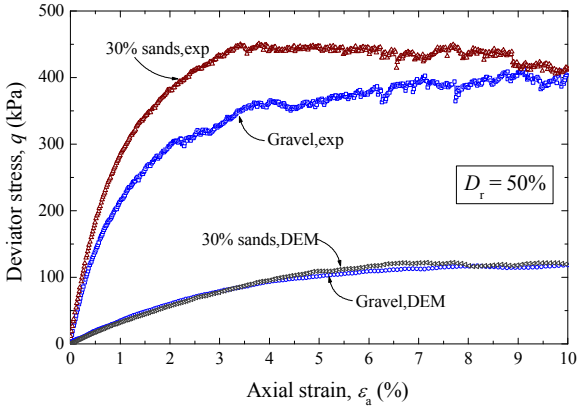

Fig. 11: Comparison of deviator stress vs. axial strain for the specimens of 50% of D_r

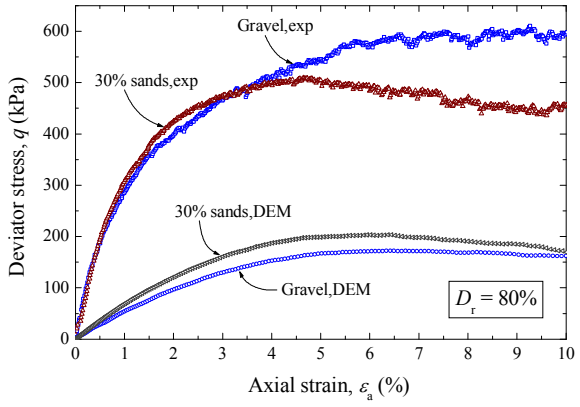

Fig. 12: Comparison of deviator stress vs. axial strain for the specimens of 80% of D_r

Fig. 13 shows failure friction angle, ϕ_f, vs. dry density, ρ_d, of sand-gravel specimens from laboratory triaxial compression tests. As shown in Fig. 13, the highest ρ_d was observed for the specimen of 50% sands in both 50% and 80% of D_r cases. In case of 80% of D_r, the gravel specimen has the largest ϕ_f, which gradually decreased until the sand specimen. However, in case of 50% of D_r, ϕ_f increases until the specimen of 30% sands, then decreased until the sand specimen. Fig. 14 shows ϕ_f vs. ρ_d for DEM-simulated specimens. As shown in Fig. 14, overall, both ρ_d and ϕ_f increased with %sands (up to 30% sands) and reached peak values for the specimens of 30% sands in 80% of D_r. In case of 50% of D_r, ϕ_f remains same for the specimens of 0% - 30% sands, then, decreased for the specimen of 50% sands and then remains same until the sand specimen same as 80% of D_r. The results showed that mixing of sands in gravel (i.e., mixing of fines in ballast) change failure frictional angle and dry density of the mixtures.

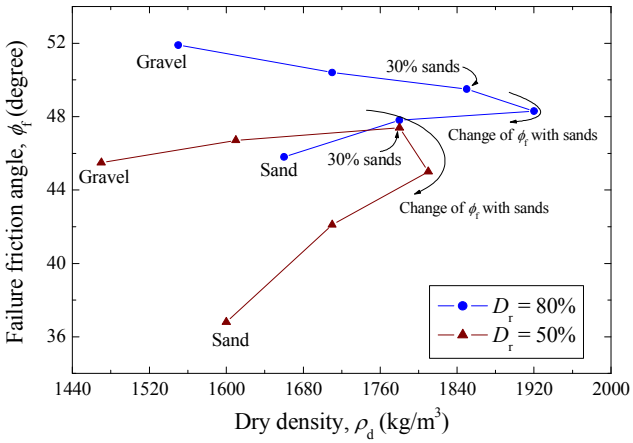

Fig. 13: Change of failure friction angle of sand-gravel specimens with sands from laboratory experiments

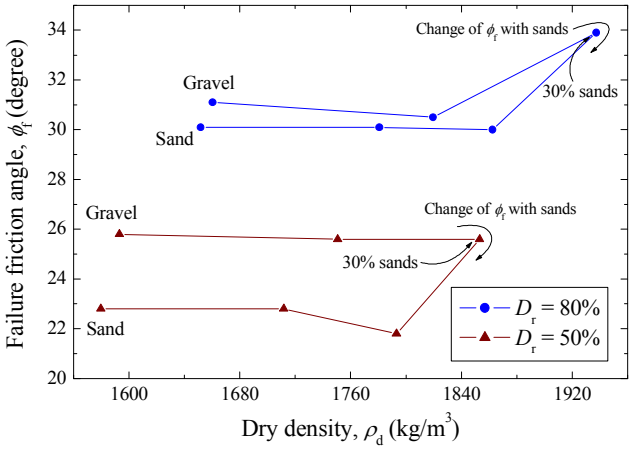

Fig. 14: Change of failure friction angle of sand-gravel specimens with sands from DEM simulations

4. CONCLUSION

Triaxial compression tests were conducted on sand-gravel mixtures to study effects of fine material mixings in ballast in railway tracks. Triaxial tests were conducted in the laboratory and in Yade, a DEM approach as the numerical simulations. Triaxial compression tests were conducted on the specimens of 50% and 80% of relative densities. The following conclusions were made,

- Void ratios (both e_{max} and e_{min}) decreased with initial addition of sands. After reaching a minimum value, void ratios increase with sands. The minimum value of void ratios in DEM simulations were observed on the specimens of 30% sands while it was 50% sands for laboratory specimens.
- Void ratios observed in DEM simulations were smaller than those of laboratory specimens. The difference in void ratios can be attribute to difference in particle shapes in DEM simulations and laboratory experiments. However, relations of void ratio change with %sands were approximately same in DEM simulations and laboratory specimens.
- The results also showed that void ratios can be simulated in DEM simulations same as those of laboratory experiments for specimens of small particles (e.g., sands).
- As an overall finding, in both laboratory experiments and DEM simulations, the highest stress-strain curves were observed on the specimens of 30% sands. The results indicated that specimens with smaller void ratios experienced higher stress-strain curve.
- However, there is difference in stress-strain curves between the two methods, experimental specimens showing higher stress-strain curves. The difference in stress-strain curves should be attribute to difference in particle shapes in the two methods. However, on average, the results showed similar patterns in a qualitative manner.
- The specimens of 30% sands experienced the highest dry density and failure friction angle in DEM simulations. In experimental specimens, 50% sand samples showed the highest dry density. In laboratory tests, the results were not consistent for failure friction angle though.

5. ACKNOWLEDGMENT

Japanese Government is highly acknowledged for providing financial assistance through Monbukagakusho scholarship to the first author to study in Yokohama National University, Japan.

6. REFERENCES

[1] Thakur PK, Vinod JS and Indraratna B., Effect of particle breakage on cyclic densification of ballast: a DEM approach, In Proc., IOP Conf. Series: Materials Science and Engineering, 2010, pp. 122-129.

[2] Raymond GP, Reinforced ballast behaviour subjected to repeated load, Geotextiles and Geomembranes, vol. 20, 2002, pp. 39-61.

[3] Indraratna B, Khabbaz H, Salim W and Christie D, Geotechnical properties of ballast and the role of geosynthetics in rail track stabilization, Journal of Ground Improvement, vol. 10, No. 3, 2006, pp. 91-102.

[4] Cundal PA and Strack ODL, A discrete numerical model for granular assemblies, Geotechnique, vol. 29, No. 1, 1979, pp. 47-65.

[5] Smilauer V, Catalano E, Chareyre B, Dorofeenko S, Duriez J, Gladky A, Kozicki J, Modenese C, Scholtes L, Sibille L, Stransky J, Thoeni K (2010), Yade Reference Documentation, In Yade Documentation (V. Smilauer, ed.), The Yade Project, 1st ed. (http://yade-dem.org/doc/).

[6] Widulinski L, Kozicki J and Tejchman J, Numerical simulations of triaxial test with sand using DEM, Archives of Hydro-Engineering and Environmental Mechanics, vol. 56, No. 3-4, 2009, pp. 149-171.

[7] Sayeed MA, Suzuki K and Rahman MM, Strength and deformation characteristics of granular materials under extremely low to high confining pressures in triaxial compression, International Journal of Civil & Environmental Engineering, vol. 11, No. 4, 2011, pp. 1-6.

[8] JIS A 1224, Test method for minimum and maximum densities of sands, 2009.

[9] JGS 0527, Method for triaxial compression test on unsaturated soils, 1998.

[10] Goto SF, Tastuoka F, Shibuya S, Kim YS and Sato T, A simple gauge for local small strain measurements in the laboratory, Soils and Foundations, vol. 31, No. 1, 1991, pp. 169-180.

[11] JIS A 1204, Test method for particle size distribution of soils, 2009.

[12] Lade PV, Liggio CD and Yamamuro JA, Effect of non-plastic fines on minimum and maximum void ratios of sand, Geotechnical Testing Journal, ASTM, vol. 21, No. 4, 1998, pp. 336-347.

[13] Lin X and Ng TT, A three-dimensional discrete element model using arrays of ellipsoids, Geotechnique, vol. 47, No. 2, 1997, pp. 319-329.

[14] Yan G, Sui YH and Glenn M, Simulation of granular material behaviour using DEM, In Proc., 6th International Conference on Mining Science & Technology, 2009, pp. 598-605.

Int. J. of GEOMATE, June, 2013, Vol. 4, No. 2 (Sl. No. 8), pp. 546-551.
MS No. 53 received July 12, 2012, and reviewed under GEOMATE publication policies.
Copyright © 2013, International Journal of GEOMATE. All rights reserved, including the making of copies unless permission is obtained from the copyright proprietors. Pertinent discussion including authors' closure, if any, will be published in the June 2014 if the discussion is received by Dec., 2013.
Corresponding Author: Janaka Kumara